Chemistry–A European Journal
Research Article
doi.org/10.1002/chem.202203941
Chemistry Europe
European Chemical Societies Publishing
www.chemeurj.org

Chemo-Enzymatic Synthesis of Long-Chain Oligosaccharides for Studying Xylan-Modifying Enzymes

Ignacio Álvarez-Martínez,[a, b] Colin Ruprecht,[a, b] Deborah Senf,[b] Hsin-tzu Wang,[c, d, e] Breeanna R. Urbanowicz,[c, d] and Fabian Pfrengle*[a, b]

Abstract: Plant research is hampered in several aspects by a lack of pure oligosaccharide samples that closely represent structural features of cell wall glycans. An alternative to purely chemical synthesis to access these oligosaccharides is chemo-enzymatic synthesis using glycosynthases. These enzymes enable the ligation of oligosaccharide donors, when activated for example as α-glycosyl fluorides, with suitable acceptor oligosaccharides. Herein, the synthesis of xylan oligosaccharides up to dodecasaccharides is reported, with glycosynthase-mediated coupling reactions as key steps. The xylo-oligosaccharide donors were protected at the non-reducing end with a 4-*O*-tetrahydropyranyl (THP) group to prevent polymerization. Installation of an unnatural 3-*O*-methylether substituent at the reducing end xylose of the oligosaccharides ensured good water solubility. Biochemical assays demonstrated enzymatic activity for the xylan acetyltransferase XOAT1 from *Arabidopsis thaliana*, xylan arabinofuranosyltransferase XAT3 enzymes from rice and switchgrass, and the xylan glucuronosyltransferase GUX3 from *Arabidopsis thaliana*. In case of the glucuronosyltransferase GUX3, MALDI-MS/MS analysis of the reaction product suggested that a single glucuronosyl substituent was installed primarily at the central xylose residues of the dodecasaccharide acceptor, demonstrating the value of long-chain acceptors for assaying biosynthetic glycosyltransferases.

Introduction

All plant cells are surrounded by a polysaccharide-rich wall that constitutes the majority of the terrestrial biomass on Earth and thus play important roles for both the environment and economy.[1] The hemicellulose xylan is the second most abundant polysaccharide after cellulose in these walls,[2] and plants incorporate approximately 10 billion tons of carbon each year into this polysaccharide alone.[2,3] Xylans are a major component of everyday food and forage, playing a central role in human and animal health. As xylans constitute up to 30% of woody biomass,[4] they are also highly relevant for the feed, paper, and biofuel industries. Specific non-food applications range from their use as oxygen barrier films for packaging to strengtheners in paper production.[5] The molecular composition and primary structure of xylan polymers have a strong impact on the macroscopic properties of plant tissues, and can significantly vary between plant species and tissues. Xylans in land plants possess a common backbone consisting of β-1,4-linked D-xylopyranosyl residues (Figure 1A). In both hardwoods and softwoods, the 2-position of xylose may be appended with D-glucuronic acid or 4-*O*-methylated D-glucuronic acid substituents (glucuronoxylans).[6] In contrast, the xylans present in grasses are mainly substituted with α-L-arabinofuranosyl residues in the 2- and/or 3-position, and are less frequently substituted with glucuronic acid (glucuronoarabinoxylan[7]). Furthermore, most xylans are decorated with significant amounts of regularly or irregularly spaced acetyl groups.

Like most polysaccharides, xylans are synthesized by glycosyltransferases (GTs) that use sugar nucleotides as donors to attach monosaccharides to the glycan acceptor.[8] Direct biochemical evidence has demonstrated that the β-1,4-D-xylan backbone is synthesized from UDP-xylose by xylan synthase enzymes (XYS) that are classified as members of the GT47 family in the carbohydrate active enzyme (CAZy) database.[9] The synthesis of complex xylans found in plants requires additional enzymes, and several responsible for catalyzing formation of most common substituents have been identified. For example,

[a] *I. Álvarez-Martínez, Dr. C. Ruprecht, Prof. Dr. F. Pfrengle*
Department of Chemistry
University of Natural Resources and Life Sciences Vienna
Muthgasse 18, 1190 Vienna (Austria)
E-mail: fabian.pfrengle@boku.ac.at
[b] *I. Álvarez-Martínez, Dr. C. Ruprecht, Dr. D. Senf, Prof. Dr. F. Pfrengle*
Department of Biomolecular Systems
Max Planck Institute of Colloids and Interfaces
Am Mühlenberg 1, 14476 Potsdam (Germany)
[c] *Dr. H.-t. Wang, Prof. Dr. B. R. Urbanowicz*
Department of Biochemistry and Molecular Biology
University of Georgia
Athens, GA, 30602 (USA)
[d] *Dr. H.-t. Wang, Prof. Dr. B. R. Urbanowicz*
Complex Carbohydrate Research Center
University of Georgia
Athens, GA, 30602 (USA)
[e] *Dr. H.-t. Wang*
Current address: Joint BioEnergy Institute
Emeryville, CA, 94608 (USA)

Supporting information for this article is available on the WWW under https://doi.org/10.1002/chem.202203941

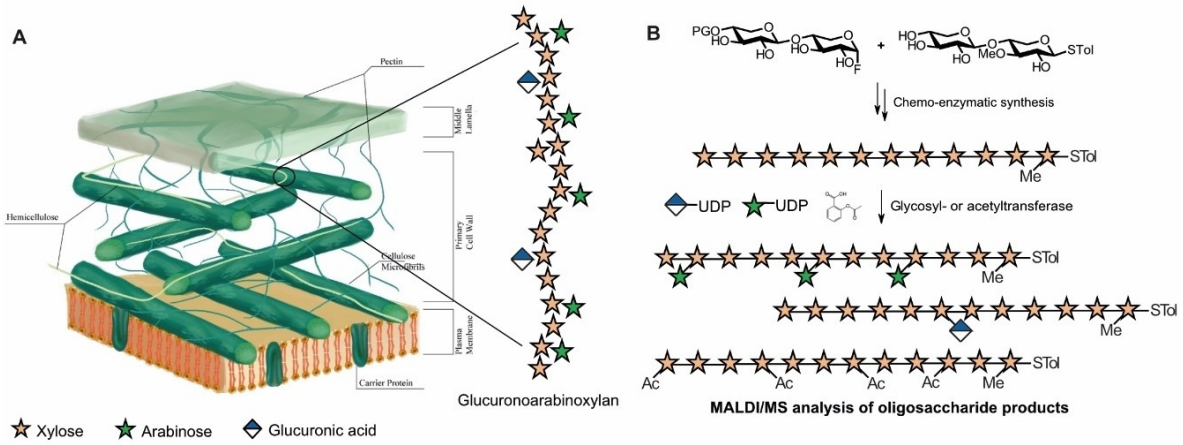

Figure 1. A) Schematic representation of the primary cell wall and the hemicellulose glucuronoarabinoxylan (GAX). B) Overview of the chemo-enzymatic synthesis scheme of long-chain oligosaccharides for use as acceptor substrates for xylan-directed glycosyl- and acetyltransferases. Structures of reaction products generated by glycosyl- and acetyltransferases are cartoon representations and the distribution of substituent structures included as a visual aid are not verified final product structures.

α-glucuronosyltransferases encoded by GLCA SUBSTITUTION OF XYLAN (GUX) genes from family GT8 add glucuronic acid (GlcA) to dicot xylan,[6b,10] xylan arabinosyltransferases (XATs) from family GT61 add arabinofuranose (Ara*f*) to xylan in grasses,[11] and xylan *O*-acetyltransferases (XOATs) from the Trichome Birefringence-Like (TBL) protein family acetylate xylan.[9b,12]

In the cell wall, the degree of polymerisation (DP) of a typical xylan polymer can reach hundreds of residues. Accordingly, during polysaccharide synthesis in the Golgi, the rapid addition of glycosyl and non-glycosyl substituents to the nascent backbone maintains solubility and inhibits assembly and interaction of the backbone residues to form aggregates.[13] As interest in elucidating the biochemical pathways responsible for cell wall polymers has grown, it has become clear that studies into the biochemical characterization of GTs that are responsible for catalyzing the addition of substituents to the polysaccharide backbone require longer, more biosimilar oligosaccharide fragments of the backbone as pseudo acceptor substrates.[14] However, the currently available oligosaccharides may be shorter or of similar length to the structural motif recognized by the respective GT, potentially yielding misleading biochemical results. Furthermore, the use of sub-optimal pseudo-substrates to study saccharide synthesis can limit or even prevent enzymatic activity, ultimately limiting information on the substitution patterns obtained.

Chemical synthesis in solution has provided xylan oligosaccharides up to a decasaccharide. Furthermore, using automated glycan assembly (AGA), linear xylan oligosaccharides up to an octasaccharide as well as different arabinosyl-substituted xylan oligosaccharides have been prepared. The synthesis of longer xylan oligosaccharides has not been reported. Removal of protecting groups following the assembly of long homo-oligomeric glycans can be problematic[15] due to limited solubility of intermediary formed semi-protected compounds that form supramolecular assemblies.[16] Enzymatic strategies may provide a solution to this issue, if the desired unprotected products are directly obtained from smaller reactants.

Here, we report the chemo-enzymatic synthesis of xylan oligosaccharides up to dodecasaccharides (DP12), with and without 3-*O*-methylation of the reducing end xylose, which enhances solubility for biochemical assays. Our strategy is based on glycosynthase-mediated coupling reactions of synthetic oligoxyloside fluorides with suitable oligoxyloside acceptors, providing a promising alternative to purely chemical synthesis. The prepared oligosaccharides were used as acceptor substrates in assays with both glycosyl- and acetyltransferases, demonstrating the importance of the substrate's chain length (Figure 1B).

Results and Discussion

In addition to chemical synthesis, a plethora of enzymes can be used to form glycosidic bonds.[17] They provide precise stereoselective control over the reactions and avoid the need for multiple protection and deprotection events. Particularly promising for the preparation of large homo-oligomeric glycan structures are glycosynthases derived from endo-glycosidases.[18] These enzymes are obtained by site-directed mutagenesis of the catalytic nucleophilic residue in endo-glycosidases. Since the natural endo-glycosidases catalyze the hydrolysis of internal glycosidic bonds in oligo- and polysaccharides, their glycosynthase counterparts enable ligation of oligosaccharides. XynAE265G (also named XT6E265G) is a xylan glycosynthase that results from the substitution of the nucleophilic glutamic acid by glycine in the active site of the extracellular *endo*-1,4-β-xylanase of *G. stearothermophilus* (XT6; family GH10).[19] This modification maintains the topology of the active site that allows stabilization of the developing charges during transition state formation[20] but prevents cleavage of the glycosidic bond. When an α-xylosyl fluoride and a xylosyl

acceptor are accommodated in the active site, their coupling reaction is catalyzed by the stabilizing interactions provided in the active site.

Starting from xylobioside building blocks (BBs) **1**[21] and **2**, long-chain xylan oligosaccharides, with or without a methylation at the reducing end xylose unit, were synthesized using chemoenzymatic iterative synthesis (Scheme 1). To generate disaccharide acceptors **3** and **4** for subsequent glycosynthase-mediated coupling reactions, the benzoyl esters in **1** and **2** were removed by methanolysis. Disaccharide α-xylosyl fluoride donor **5** was prepared by treatment of thioglycoside **1** with HF/py and NIS in DCM at −50 °C to −5 °C, followed by THP-protection of the hydroxy group and careful removal of the benzoate esters using catalytic amounts of sodium methoxide in methanol at 0 °C. After workup with Et_2O/H_2O and lyophilization of the aqueous phase, xylosyl donor **5** was obtained. In the first of the three steps, excess HF/py-solution drives the reaction to the thermodynamically favored α-xyloside. Incubation of acceptors **3** or **4** with donor **5** and glycosynthase XynAE265G afforded tetra-xylosides **6** or **7** in good yields. As the products partly precipitated during the course of the reaction, pure product could be collected by centrifugation. Additional product remaining in solution was purified by size-exclusion chromatography (see Supporting Information). The THP-group

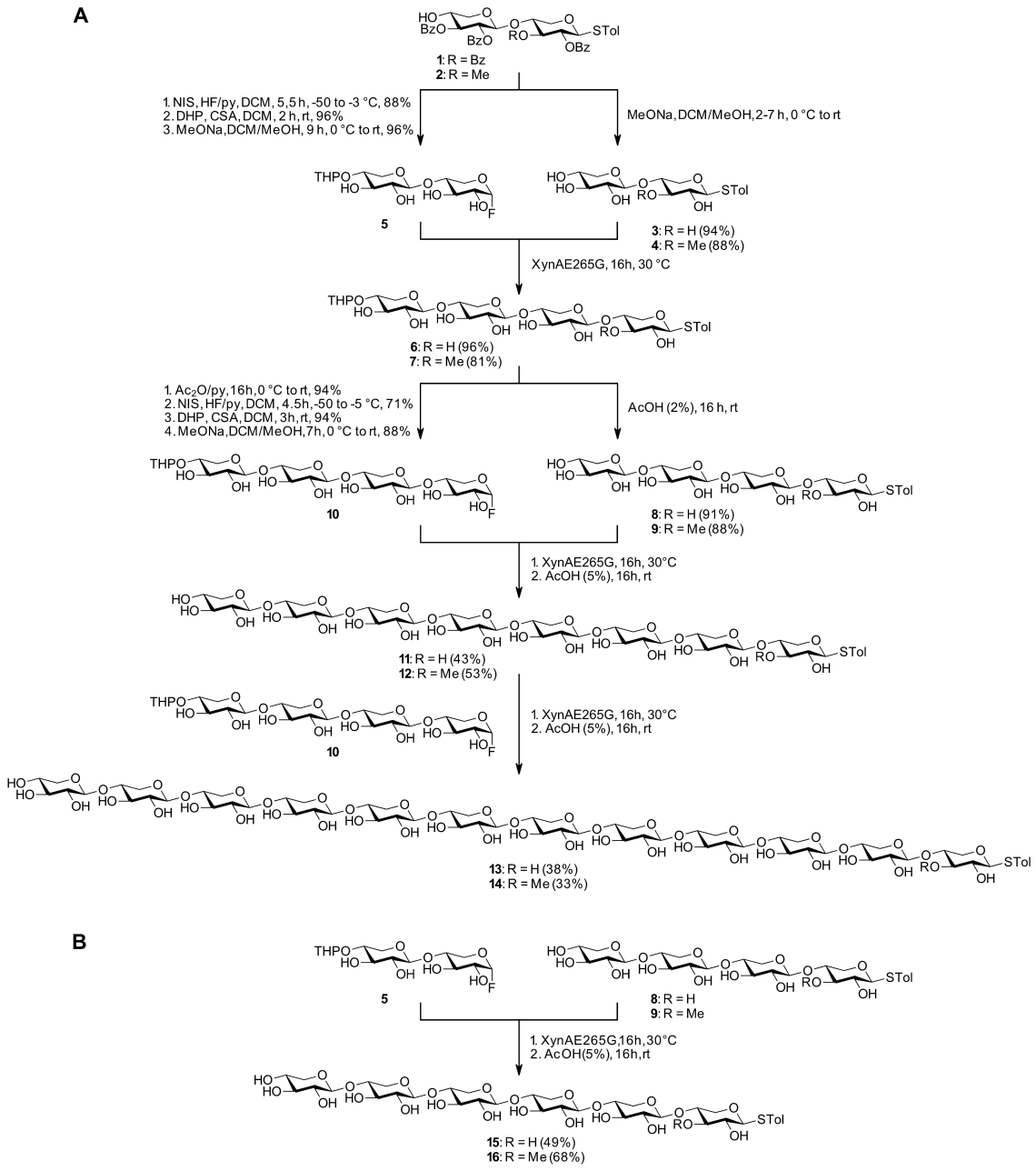

Scheme 1. A) Chemo-enzymatic synthesis of non-methylated and methylated dodeca-xylosides **13** and **14** using xylan glycosynthase XynAE265G. B) Synthesis of hexa-xylosides **15** and **16**.

prevented glycosynthase-catalyzed self-condensation of the donor.[21] Subsequently, the corresponding tetrasaccharide donor (**10**) and tetrasaccharide acceptors (**8** and **9**) were prepared. Simple acidic treatment of **6** and **7** with AcOH (5% in water) provided deprotected acceptors **8** and **9**. Formation of the tetrasaccharide donor **10** was realized by a four-step procedure, consisting of peracetylation with acetic anhydride in pyridine, fluorination using NIS and HF/py in DCM at −50 °C to −5 °C, with concomitant loss of the THP-group, re-installation of THP using dihydropyrane (DHP) and catalytic amounts of CSA, and final removal of the acetyl groups by methanolysis at 0 °C. Partial precipitation of the product upon neutralization of the basic solution provided crystalline fluoride donor **10**. Without any further purification, careful concentration of the neutral solution provided the remaining fluoride donor **10**. Alternative protecting groups to THP (PMB (*p*-methoxybenzyl), Nap (2-naphthylmethyl) and allyl) have been explored to avoid the necessity of protecting group re-installation after the fluorination step but did not provide superior results. Both PMB and Nap protecting groups were cleaved under fluorinating conditions (NIS and HF/py in DCM), even when lower temperatures were used, and the allyl group underwent iodofluorination.[22] Glycosynthase-mediated coupling of donor **10** with acceptors **8** and **9** followed by THP-removal provided octa-xylosides **11** and **12**, which were elongated to dodecasaccharides **13** and **14** with tetrasaccharide donor **10**. Additionally, reaction of disaccharide donor **5** with tetrasaccharides **8** and **9** afforded hexasaccharides **15** and **16**. As expected, the solubility of the oligo-xylosides decreased with increasing chain length, with the non-methylated dodecasaccharide **13** being almost completely insoluble in pure water. The enzymatic coupling products still furnished with a THP group were consistently less water soluble than the respective oligosaccharides obtained after THP removal. THP-deprotection of the dodecasaccharides was possible in aqueous solution after prior lyophilization from DMSO.

The assembly of architecturally complex structures such as the plant cell wall depends on the action of glycan-biosynthetic enzymes, including glycosyltransferases, acetyltransferases, and methyltransferases. With the synthesized long-chain oligosaccharides in hand, the ability of different heterologously expressed xylan-modifying enzymes to add glycosyl- and acetyl-substituents to the xylan backbone was investigated. Methylated dodecasaccharide **14** was chosen as the acceptor substrate over the respective non-methylated oligosaccharide **13**, due to its superior solubility in water. The following enzymes were investigated: i) the well-characterized acetyltransferase *At*XOAT1 (from *A. thaliana*), which served as a proof-of-principle; ii) two arabinosyltransferases from grasses, *Os*XAT3 (from *Oryza sativa*; rice) and *Pv*XAT3 (from *Panicum virgatum*; switchgrass); and iii) glucuronosyltransferase *At*GUX3 (from *A. thaliana*), whose activity had not been previously studied in vitro.

The catalytic domain of *At*XOAT1, which acetylates the 2-position of xylose units in the backbone,[23] was expressed in HEK293 cells following previously described protocols. Incubation of **14** with acetylsalicylic acid and XOAT1 for 16 h resulted in the formation of xylan oligosaccharides with five to ten acetyl groups attached to the xylose residues, as determined by MALDI mass spectrometry (Figure 2). Next, the catalytic domains of *Os*XAT3 and *Pv*XAT3 were expressed. These enzymes belong to the GT61 family, containing several glycosyltransferases involved in the 3-*O*-Ara*f* substitution of grass xylan, including multiple xylan arabinofuranosyl-transferases (XATs) from rice and wheat (*Os*XAT2-7, and *Ta*XAT1-2[11a,24]). Here, we have demonstrated the ability of XAT3 to transfer Ara*f* from UDP-Ara*f* to long xylan oligosaccharides. While *Os*XAT3 transferred up to two Ara*f* to synthetic dodeca-xyloside **14**, *Pv*XAT3 transferred up to five Ara*f* substituents (Figure 2A), reflecting the ability of grass XATs to generate highly substituted arabinoxylan polysaccharides. Finally, we expressed for the first time the catalytic domain of *At*GUX3. Substitution of xylan with glucuronic acid in dicot secondary cell walls requires two GT8 enzymes in Arabidopsis: GUX1 and GUX2, which were reported to generate strikingly different substitution patterns in vivo.[25] More recently, GUX3 was identified as the only glucuronyltransferase required for glucuronylation of Arabidopsis primary cell wall xylan.[26] The comparison of xylan oligosaccharides released from cell walls of *gux3* and *gux1/gux2* knock-out mutants suggested that GUX3 produces a unique substitution pattern, in which every sixth xylose residue carries a glucuronic acid. However, biochemical characterization and confirmation of enzymatic activity for *At*GUX3 had not been carried out. Incubation of dodecasaccharide **14** with the catalytic domain of *At*GUX3 demonstrated that GUX3 was able to transfer one equivalent of GlcA from UDP-GlcA to the synthetic oligosaccharide acceptor **14** (Figure 2A).

To determine the positions along the backbone of the pseudo-acceptor to which GUX3 added the GlcA substituent, we used matrix-assisted laser desorption/ionization-time-of-flight (MALDI-TOF) mass spectrometry (MS)/MS. Our data shows that GUX3 specifically adds GlcA to one of the two middle xylose residues of the 12mer, i.e. the 6th or 7th xylose from the non-reducing end. This finding is based on the relative abundance of the corresponding B- and Y fragments[27] (Figure 2B). These two types of fragments are the result of glycosidic bond cleavage. The resulting fragment towards the non-reducing end is the B-fragment, and the fragment towards the reducing end is the Y-fragment. The sub-index assigned to the letters B and Y represents the number of sugar units in the given fragment. Since the Y-fragments include an STol at the reducing end, they are readily identified and cannot be mistaken by internal fragments formed through cleavage of multiple glycosidic bonds. Given that the GlcA residue can be cleaved off during fragmentation, as observed for the unsubstituted Y_{12}-fragment (the most intense peak in the spectrum), the GlcA-containing Y-fragments (blue) represent the most reliable source of information. Of these, the smallest is the GlcA-substituted Y_6-fragment, suggesting that no GlcA-substitutions are present on the five xylose units towards the reducing end. Furthermore, unsubstituted Y-fragments with seven (Y_7) or more xylose units (red) were found to be of low abundance, suggesting that substitution is primarily present at the 6th or 7th xylose unit and not at the five xylose residues towards the non-reducing end. These observations are supported by the

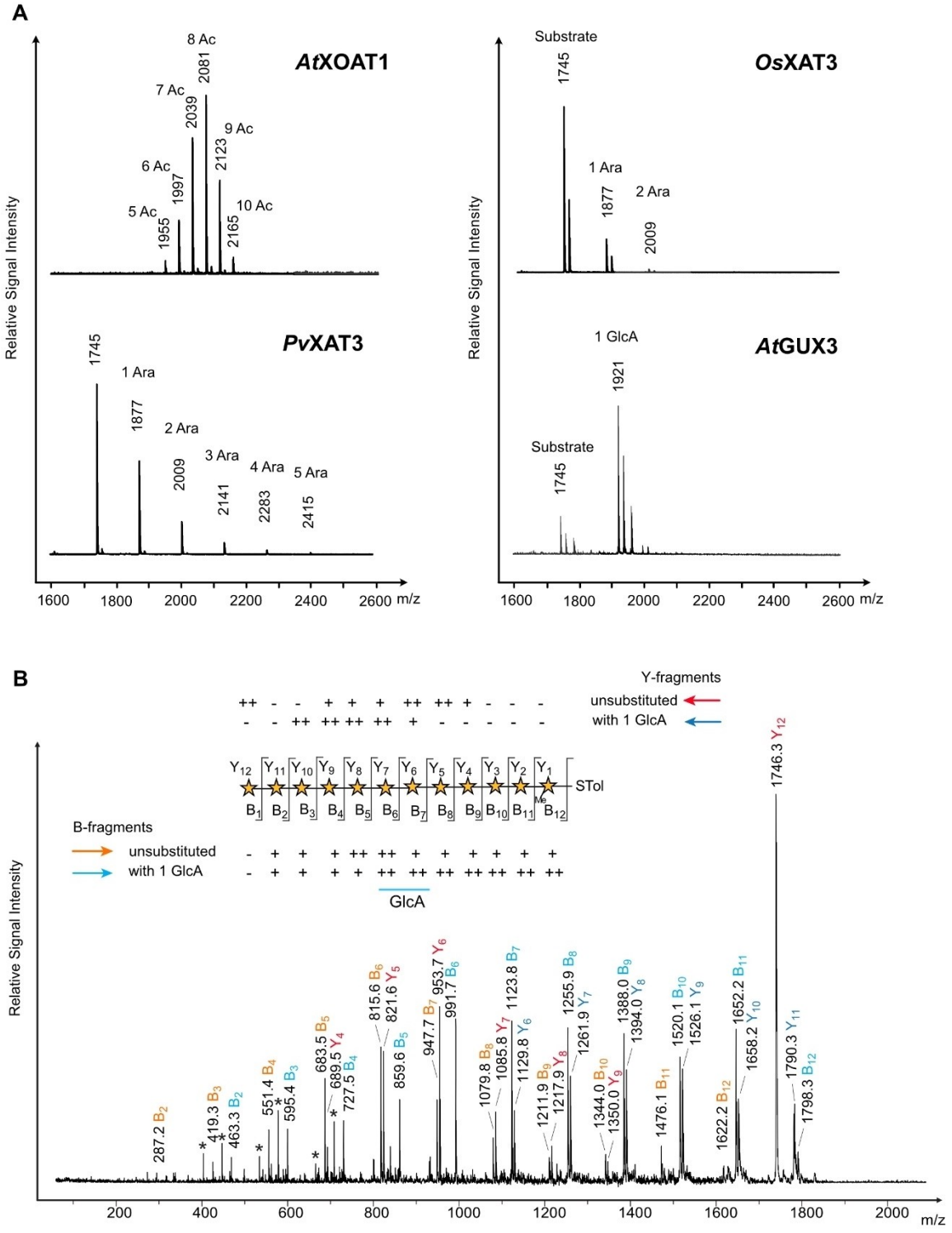

Figure 2. MALDI-TOF MS analysis of glycosyltransferase reactions (16 h incubation) with oligosaccharide **14** as a glycosyl acceptor substrate (see Figure 1B for an illustration). A) The arabinosyltransferases *Os*XAT3 from rice and *Pv*XAT3 from switchgrass show different degree of arabinosylation of the xylan 12mer. *At*XOAT1 from Arabidopsis can catalyze the transfer of up to ten acetyl groups to the xylan backbone. Analysis of *At*GUX3 reactions products showed the enzyme is able to catalyze the attachment of precisely one glucuronic acid to the xylo-oligomer. Indicated masses correspond to the Na^+ adducts. B) MALDI-TOF MS/MS analysis of the *At*GUX3 product with the parent mass 1921. Y-fragments represent thioglycosides including the original reducing end (with STol), whereas the B-fragments include the non-reducing end of the 12mer. The Y12 fragment originates from the detachment of the GlcA residue during fragmentation. The proposed predominant glycosylation sites for GUX3 are indicated with a blue line. Indicated masses correspond to the Na^+-adducts of the fragments. Asterisks denote H^+ adducts of the adjacent fragments (Na^+-adduct mass −22).

observed B-fragments. Unsubstituted B-fragments containing eight (B_8) or more xylose units (yellow) are substantially less abundant, while B-fragments with five (B_5) or less xylose units are present in both substituted (light blue) and unsubstituted form (yellow). The presence of small GlcA-substituted B-fragments (light blue) may be explained by the formation of internal fragments. Still, we cannot exclude the presence of small amounts of oligosaccharides with GlcA-substitution further towards the non-reducing end. Overall, our results suggest that GUX3 requires five unsubstituted xyloses adjacent to both sides of the glycosylation site to install a single GlcA residue, converting almost all of the acceptor to the glucuronosylated form. This is in contrast to the activity of the XOAT and XATs, which all add more than one substituent to the xylo-oligomer. This in vitro glycosylation pattern of GUX3 is in agreement with the pattern proposed to be produced in vivo. Our data therefore suggests that the GUX3 substrate specificity is sufficient to produce the xylan-substitution pattern with every 6th xylosyl residue decorated with GlcA that was observed using *gux*-mutant analyses. On the contrary, GUX1 generates specific acetylation patterns prior to glucuronosylation to guide the synthesis of the observed GlcA-substitution patterns in secondary cell wall xylan.[28] Previous attempts to show activity of GUX3 using a xylan hexamer were unsuccessful.[10] However, experiments with WT and mutant Arabidopsis microsomes from callus tissue indicated that GUX3 is involved in glucuronosylation of larger xylan oligosaccharides.[26] It remained unclear, if GUX3 is an active glycosyltransferase or rather a scaffold protein in a xylan-synthesizing complex. Our finding of GUX3 activity on a xylan 12mer proves that GUX3 is active on its own and highlights the potential of using long-chain oligosaccharides for biosynthetic studies.

Conclusion

We have performed the chemo-enzymatic syntheses of two xylan dodecasaccharides, with and without an artificial methyl group at the 3-position of the reducing end xylose residue. The glycosynthase XynAE265G efficiently catalyzed the reaction between two defined xylo-oligosaccharides, a glycosyl fluoride donor and a thioglycoside acceptor. To prevent polymerization, the 4-OH of the donor's non-reducing xylose residue was protected with a THP group. By applying further enzymatic coupling cycles, the presented strategy may provide an easy access to even larger xylan oligosaccharides for biosynthetic studies. The presented strategy may be particularly competitive to purely chemical synthesis for large oligosaccharides where lower yields in the glycosylation reactions and increasing difficulties in the deprotection of the final oligosaccharide may be observed.

The more water-soluble methylated dodecasaccharide was used as an acceptor substrate to analyze the xylan-modifying enzymes *At*XOAT1, *Os*XAT3, *Pv*XAT3 and *At*GUX3. We showed in vitro activity for heterologously expressed *At*GUX3 for the first time and observed that *At*GUX3 added a single glucuronyl substituent to one of the central xylose residues of the acceptor, indicating that, unlike *At*GUX1, *At*GUX3 alone is capable of producing the regular substitution pattern observed in vivo. The length of the used oligosaccharide was an important determinant to detect activity and to analyze substrate specificity.

Experimental Section

General information: Solvents and reagents were used as supplied without further purification. Anhydrous solvents were taken from a dry solvent system (JC-Meyer Solvent Systems) or used directly from the supplier. Column chromatography was carried out using Fluka silica gel 60 (230–400 mesh). NMR spectra were recorded on a Bruker Avance III 600 or a Bruker 400 instrument spectrometer using solutions of the respective compound in $CDCl_3$, DMSO-d_6 or D_2O. NMR chemical shifts (δ) are reported in ppm and coupling constants (*J*) in Hz. ^{1}H spectra were referenced to 7.26 ($CDCl_3$) and 0.00 (D_2O, external calibration to sodium 3-(trimethylsilyl)propane-1-sulfonate, DSS) ppm. ^{13}C spectra were referenced to 77.16 ($CDCl_3$) and 67.19 (D_2O, external calibration to 1,4-dioxane) ppm. High resolution mass spectra were obtained on a 6210 ESI-TOF mass spectrometer (Agilent) or a Micromass Q-TOF Ultima Global instrument. For filtration, syringe filters (RC, 0.45 μm) from Roth were used. Reactions were monitored using reverse phase HPLC with a C4 column (Jupiter, 150×2 mm, Phenomenex) in a Shimadzu LC-10 system that is coupled to a Shimadzu LCMS 2020 mass spectrometer and an Alltech 3300 Evaporative Light Scattering Detector (ELSD).

General procedure A for glycosynthase-mediated reactions: α-Xylosyl fluoride donor (1.2 equiv.) and xylo-oligosaccharide acceptor (1 equiv.) were dissolved in phosphate buffer (100 mM; pH 7.4). XynAE265G[19a,29] in phosphate buffer (100 mM; pH 7.4) was added in order to reach a final concentration of 1 mg/mL. The mixture was allowed to react in a rotating shaker at 30 °C for 16 h and the desired product precipitated to varying extents. The cloudy reaction mixture was centrifuged, and the insoluble solid was dispersed twice in H_2O and centrifuged. The aqueous phases were combined and lyophilised. The solid obtained after lyophilization was dissolved in a small amount of H_2O and purified by size-exclusion chromatography (SEC) using a Bio-Gel® P-2 polyacrylamide gel with H_2O as an eluent. The compound obtained by SEC-purification was combined with the insoluble compound obtained after centrifugation to give the desired product as a white or colourless solid.

General procedure B for THP removal: The THP-protected xylo-oligosaccharide product was dissolved in water. If necessary, a small amount of DMSO was added for complete dissolution of the starting material. AcOH was added and the reaction mixture was stirred for 16 h or until the reaction was complete, as monitored by thin layer chromatography (TLC) or liquid chromatography-mass spectrometry (LC–MS) using a C4 column (Phenomenex). The reaction mixture was then lyophilised, and the residue was purified, if necessary, by size-exclusion chromatography (SEC) using Bio-Gel® P-2 polyacrylamide gel with H_2O as an eluent. The procedure yielded the desired product as a white or colourless solid.

Expression of the XynAE265G glycosynthase: The expression of XynAE265G in *E. coli* was performed as previously described.[19a,21] In brief, the XynA gene, with Glu265 mutated to Gly, was expressed in *E. coli* BL21 (DE3) using the pET9d vector. The expression of the enzyme was induced with 0.5 mM isopropyl-β-D-thiogalactopyranosid (IPTG) and after cell lysis the cell debris was removed by centrifugation at 10000 g for 45 min at 4 °C. The supernatant could be directly used for the polymerization assay, because of the high expression rate of XynAE265G, with a single major band at the

expected size of 43.8 kDa and relatively small amounts of endogenous *E. coli* proteins (for details see[21]).

Expression of the glycosyltransferases PvXAT3, OsXAT3 and AtGUX3 and the acetyltransferase AtXOAT1: The heterologous expression of the glycosyltransferases and the acetyltransferase (*At*XOAT1-cat comprising amino acids 133–487) in HEK293F cells was performed as previously described.[23,30] Plant coding sequences were amplified from a cDNA template and cloned into mammalian expression vector pGEN2-DEST according to standard protocols.[30b] Truncated versions of the coding sequences were amplified using the primers listed in Table 1 (Supporting Information) and cloned into the pDONR221 vector to generate Gateway entry clones. Using LR clonase (Invitrogen) the genes were then cloned into the pGEn2-DEST vector to generate an expression construct to yield recombinant proteins with an 8xHis tag, an AviTag, and "superfolder" GFP at the N-terminus of the truncated coding region of the respective gene. The constructs were transfected into HEK293F cells as previously described.[30b] In brief, the cells were transfected and then the protein was secreted into the culture medium during several additional days of cultivation. Soluble secreted fusion proteins were purified from the clarified culture media using HisTrap HP columns (GE Healthcare) and dialyzed into 50 mM HEPES sodium salt buffer, pH 6.8, including 5% glycerol. The concentration of the resulting proteins was measured using a NanoDrop Microvolume Spectrophotometer based on their absorbance at 280 nm.

Enzyme assays: The enzyme assays were performed using the methylated xylan 12mer **14** as acceptor substrate with the following setup: i) for *At*XOAT1: 0.5 mM oligosaccharide acceptor, 6 mM acetyl salicylic acid, 40 μM enzyme; ii) for *Os*XAT3 and *Pv*XAT3: 0.5 mM oligosaccharide acceptor, 1 mM UDP-arabinose, 20 μM enzyme; iii) for *At*GUX3: 0.5 mM oligosaccharide acceptor, 1 mM UDP-glucuronic acid, 10 μM enzyme. The reactions were adjusted to a final volume of 10 μL using 50 mM HEPES sodium salt buffer, pH 6.8. The reactions were incubated for 16 h at room temperature and then terminated by incubation for 10 min at 85 °C.

MALDI-TOF analysis: MALDI-TOF MS analysis was performed using an Autoflex Speed (Bruker Daltonics, Germany) in positive ion mode using FlexControl 3.4 software. To remove salts from the enzyme reactions, 10 μL of a suspension of AG 50W–X8 cation exchange resin (Biorad) in water was added before spotting the samples. After incubation for 10 min, the samples were centrifuged and 1 μL of the supernatant was spotted on a MALDI plate. After drying, 1 μL of 2,5-dihydroxy-benzoic acid matrix (DHB, 10 mg/mL in 50% acetonitrile/water) was added, and the plate was dried again. To identify the position of the GlcA residue in the *At*GUX3 reaction product, MALDI MS/MS experiments were performed using the LIFT cell as described previously.[31] Fragment ions of the GlcA-substituted xylan 12mer (Na^+-adduct) were generated by laser-induced dissociation (LID) in positive ion mode. Typically, 500 shots were summed for MS (reflector voltage, lens voltage and gain respectively 21 kV, 8.8 kV and 1997 V) and 4000 shots were summed for MS/MS (reflector voltage, lift voltage and gain respectively 27 kV, 19 kV and 1944 V). Spectra were processed with the manufacturer's software (Bruker Flexanalysis 3.3.80) using the SNAP algorithm.

Acknowledgements

This work was funded in part by the DFG grant PF850/7-1 to FP. Funding to BRU was provided by the Center for Bioenergy Innovation (CBI), from the U.S. Department of Energy Bioenergy Research Centers supported by the Office of Biological and Environmental Research in the DOE Office of Science. We thank the Max Planck Society for financial support. The plasmid for expression of XynAE265G was kindly provided by Prof. Dr. Yuval Shoham (Technion Israel Institute of Technology). We thank Lina Maltrovsky for technical assistance.

Conflict of Interest

The authors declare no conflict of interest.

Data Availability Statement

The data that support the findings of this study are available in the supplementary material of this article.

Keywords: carbohydrates · glycosynthase · MALDI-TOF analysis · plant cell wall · xylan biosynthesis

[1] a) N. C. Carpita, M. C. McCann, *J. Biol. Chem.* **2020**, *295*, 15144–15157; b) Y. M. Bar-On, R. Phillips, R. Milo, *Proc. Natl. Acad. Sci. USA* **2018**, *115*, 6506–6511.
[2] P. J. Smith, H. T. Wang, W. S. York, M. J. Pena, B. R. Urbanowicz, *Biotechnol. Biofuels* **2017**, *10*.
[3] a) J. M. Melillo, A. D. Mcguire, D. W. Kicklighter, B. Moore, C. J. Vorosmarty, A. L. Schloss, *Nature* **1993**, *363*, 234–240; b) M. Pauly, K. Keegstra, *Curr. Opin. Plant Biol.* **2010**, *13*, 305–312.
[4] T. E. Timell, *Wood Sci. Technol.* **1967**, *1*, 45–70.
[5] a) A. Escalante, A. Goncalves, A. Bodin, A. Stepan, C. Sandstrom, G. Toriz, P. Gatenholm, *Carbohydr. Polym.* **2012**, *87*, 2381–2387; b) F. G. Kong, Y. Q. Guo, Z. M. Liu, S. J. Wang, L. A. Lucia, *BioResources* **2018**, *13*, 2960–2976.
[6] a) H. V. Scheller, P. Ulvskov, *Ann. Rev. Plant. Biol.* **2010**, *61*, 263–289; b) J. C. Mortimer, G. P. Miles, D. M. Brown, Z. Zhang, M. P. Segura, T. Weimar, X. Yu, K. A. Seffen, E. Stephens, S. R. Turner, P. Dupree, *Proc. Natl. Acad. Sci. USA* **2010**, *107*, 17409–17414.
[7] J. Vogel, *Curr. Opin. Plant Biol.* **2008**, *11*, 301–307.
[8] L. L. Lairson, B. Henrissat, G. J. Davies, S. G. Withers, *Annu. Rev. Biochem.* **2008**, *77*, 521–555.
[9] a) J. K. Jensen, N. R. Johnson, C. G. Wilkerson, *Plant J.* **2014**, *80*, 207–215; b) B. R. Urbanowicz, M. J. Pena, H. A. Moniz, K. W. Moremen, W. S. York, *Plant J.* **2014**, *80*, 197–206.
[10] E. A. Rennie, S. F. Hansen, E. E. Baidoo, M. Z. Hadi, J. D. Keasling, H. V. Scheller, *Plant Physiol.* **2012**, *159*, 1408–1417.
[11] a) N. Anders, M. D. Wilkinson, A. Lovegrove, J. Freeman, T. Tryfona, T. K. Pellny, T. Weimar, J. C. Mortimer, K. Stott, J. M. Baker, M. Defoin-Platel, P. R. Shewry, P. Dupree, R. A. Mitchell, *Proc. Natl. Acad. Sci. USA* **2012**, *109*, 989–993; b) R. Q. Zhong, D. T. Cui, D. R. Phillips, N. T. Sims, Z. H. Ye, *Planta* **2021**, *254*.
[12] a) M. Pauly, V. Ramirez, *Front. Plant Sci.* **2018**, *9*; b) R. Zhong, D. Cui, Z. H. Ye, *Plant Cell Physiol.* **2017**, *58*, 2126–2138.
[13] J. Berglund, D. Mikkelsen, B. M. Flanagan, S. Dhital, S. Gaunitz, G. Henriksson, M. E. Lindstrom, G. E. Yakubov, M. J. Gidley, F. Vilaplana, *Nat. Commun.* **2020**, *11*.
[14] a) F. Pfrengle, *Curr. Opin. Chem. Biol.* **2017**, *40*, 145–151; b) C. Ruprecht, M. Blaukopf, F. Pfrengle, *Curr. Opin. Chem. Biol.* **2022**, *71*, 102208.
[15] M. Delbianco, A. Kononov, A. Poveda, Y. Yu, T. Diercks, J. Jimenez-Barbero, P. H. Seeberger, *J. Am. Chem. Soc.* **2018**, *140*, 5421–5426.
[16] Y. Yu, S. Gim, D. Kim, Z. A. Arnon, E. Gazit, P. H. Seeberger, M. Delbianco, *J. Am. Chem. Soc.* **2019**, *141*, 4833–4838.
[17] a) R. Heinzler, T. Fischoder, L. Elling, M. Franzreb, *Adv. Synth. Catal.* **2019**, *361*, 4506–4516; b) L. Liu, A. R. Prudden, C. J. Capicciotti, G. P. Bosman, J. Y. Yang, D. G. Chapla, K. W. Moremen, G. J. Boons, *Nat. Chem.* **2019**, *11*, 161–169; c) K. W. Moremen, A. Ramiah, M. Stuart, J. Steel, L. Meng, F. Forouhar, H. A. Moniz, G. Gahlay, Z. W. Gao, D. Chapla, S. Wang, J. Y.

Yang, P. K. Prabhakar, R. Johnson, M. dela Rosa, C. Geisler, A. V. Nairn, J. Seetharaman, S. C. Wu, L. Tong, H. J. Gilbert, J. LaBaer, D. L. Jarvis, *Nat. Chem. Biol.* **2018**, *14*, 156-++.
[18] a) M. R. Hayes, J. Pietruszka, *Molecules* **2017**, *22*; b) L. F. Mackenzie, Q. P. Wang, R. A. J. Warren, S. G. Withers, *J. Am. Chem. Soc.* **1998**, *120*, 5583–5584; c) S. Shoda, H. Uyama, J. Kadokawa, S. Kimura, S. Kobayashi, *Chem. Rev.* **2016**, *116*, 2307–2413; d) P. J. Smith, M. E. Ortiz-Soto, C. Roth, W. J. Barnes, J. Seibel, B. R. Urbanowicz, F. Pfrengle, *ACS Sustainable Chem. Eng.* **2020**, *8*, 11853–11871.
[19] a) A. Ben-David, T. Bravman, Y. S. Balazs, M. Czjzek, D. Schomburg, G. Shoham, Y. Shoham, *ChemBioChem* **2007**, *8*, 2145–2151; b) A. Teplitsky, A. Mechaly, V. Stojanoff, G. Sainz, G. Golan, H. Feinberg, R. Gilboa, V. Reiland, G. Zolotnitsky, D. Shallom, A. Thompson, Y. Shoham, G. Shoham, *Acta Crystallogr. Sect. D* **2004**, *60*, 836–848.
[20] A. Warshel, P. K. Sharma, M. Kato, Y. Xiang, H. Liu, M. H. Olsson, *Chem. Rev.* **2006**, *106*, 3210–3235.
[21] D. Senf, C. Ruprecht, S. Kishani, A. Matic, G. Toriz, P. Gatenholm, L. Wagberg, F. Pfrengle, *Angew. Chem. Int. Ed. Engl.* **2018**, *57*, 11987–11992.
[22] M. Kuroboshi, T. Hiyama, *Bull. Chem. Soc. Jpn.* **1995**, *68*, 1799–1805.
[23] V. V. Lunin, H. T. Wang, V. S. Bharadwaj, M. Alahuhta, M. J. Pena, J. Y. Yang, S. A. Archer-Hartmann, P. Azadi, M. E. Himmel, K. W. Moremen, W. S. York, Y. J. Bomble, B. R. Urbanowicz, *Plant Cell* **2020**, *32*, 2367–2382.
[24] R. Zhong, D. Cui, D. R. Phillips, N. T. Sims, Z. H. Ye, *Planta* **2021**, *254*, 131.
[25] J. R. Bromley, M. Busse-Wicher, T. Tryfona, J. C. Mortimer, Z. Zhang, D. M. Brown, P. Dupree, *Plant J.* **2013**, *74*, 423–434.
[26] J. C. Mortimer, N. Faria-Blanc, X. Yu, T. Tryfona, M. Sorieul, Y. Z. Ng, Z. Zhang, K. Stott, N. Anders, P. Dupree, *Plant J.* **2015**, *83*, 413–426.
[27] B. Domon, C. E. Costello, *Glycoconjugate J.* **1988**, *5*, 397–409.
[28] N. J. Grantham, J. Wurman-Rodrich, O. M. Terrett, J. J. Lyczakowski, K. Stott, D. Iuga, T. J. Simmons, M. Durand-Tardif, S. P. Brown, R. Dupree, M. Busse-Wicher, P. Dupree, *Nat. Plants* **2017**, *3*, 859–865.
[29] A. Teplitsky, A. Mechaly, V. Stojanoff, G. Sainz, G. Golan, H. Feinberg, R. Gilboa, V. Reiland, G. Zolotnitsky, D. Shallom, A. Thompson, Y. Shoham, G. Shoham, *Acta Crystallogr. Sect. D* **2004**, *60*, 836–848.
[30] a) C. Ruprecht, M. P. Bartetzko, D. Senf, A. Lakhina, P. J. Smith, M. J. Soto, H. Oh, J. Y. Yang, D. Chapla, D. Varon Silva, M. H. Clausen, M. G. Hahn, K. W. Moremen, B. R. Urbanowicz, F. Pfrengle, *Angew. Chem. Int. Ed. Engl.* **2020**; b) P. K. Prabhakar, H. T. Wang, P. J. Smith, J. Y. Yang, W. J. Barnes, M. J. Pena, K. W. Moremen, B. R. Urbanowicz, *Methods Cell Biol.* **2020**, *160*, 145–165.
[31] a) A. Hykollari, C. I. Balog, D. Rendić, T. Braulke, I. B. Wilson, K. Paschinger, *J. Proteome Res.* **2013**, *12*, 1173–1187; b) J. Vanbeselaere, S. Yan, A. Joachim, K. Paschinger, I. B. Wilson, *Glycobiology* **2018**, *28*, 474–481.

Manuscript received: December 16, 2022
Accepted manuscript online: February 15, 2023
Version of record online: March 27, 2023